

Operational (short-term) earthquake loss forecasting in Italy

Iunio Iervolino,¹ Eugenio Chioccarelli,¹ Massimiliano Giorgio,² Warner Marzocchi,³
Giulio Zuccaro,¹ Mauro Dolce,⁴ and Gaetano Manfredi.¹

¹*Dipartimento di Strutture per l'Ingegneria e l'Architettura, Università degli Studi di Napoli Federico II, Naples, Italy. {iunio.iervolino; eugenio.chioccarelli; giulio.zuccaro; gaetano.manfredi}@unina.it*

²*Dipartimento di Ingegneria Industriale e dell'Informazione, Seconda Università degli Studi di Napoli, Aversa (CE), Italy. massimiliano.giorgio@unina2.it*

³*Istituto Nazionale di Geofisica e Vulcanologia, Rome, Italy. warner.marzocchi@ingv.it*

⁴*Dipartimento della Protezione Civile, Presidenza del Consiglio dei Ministri, Rome, Italy. mauro.dolce@protezionecivile.it*

Abstract

The seismological community is currently developing operational earthquake forecasting (OEF) systems that aim to estimate, based on continuous ground motion recording by seismic networks, the seismicity in an area of interest; the latter may be expressed, for example, in terms of rates of events exceeding a certain magnitude threshold in a short-period of time (days to weeks). OEF may be possibly used for short-term seismic risk management in regions affected by seismic swarms only if its results may be the input to compute, in a probabilistically sound manner, consequence-based risk metrics.

The present paper reports about feasibility of short-term risk assessment, or operational earthquake loss forecasting (OELF), in Italy. The approach is that of performance-based earthquake engineering, where the loss rates are computed by means of hazard, vulnerability, and exposure. The risk is expressed in terms of individual and regional measures, which are based on short-term macroseismic intensity (or ground motion intensity) hazard. The vulnerability of the built environment relies on damage probability matrices empirically calibrated for Italian structural classes, and exposure data in terms of buildings per vulnerability class and occupants per building typology. All vulnerability and exposure data are at the municipality scale.

The developed procedure, which is virtually independent of the seismological model used, is implemented in an experimental OELF system that continuously processes OEF information to produce nationwide risk maps applying to the week after the OEF data release. This is illustrated by a retrospective application to the 2012 Pollino (southern Italy) seismic sequence, which provides insights on the capabilities of the system and on the impact, on short-term risk assessment, of the methodology currently used for OEF in Italy.

33 Introduction

34 Short-term risk assessment (i.e., during seismic swarms) is emerging as a topic of increasing
35 importance because of its broad impact in terms of affected communities. A great deal of research in
36 the geophysical community is currently devoted to operational earthquake forecasting (OEF; e.g.,
37 Jordan et al., 2011), represented by the bulk of models and methods to constantly update estimates of
38 seismicity on the basis of continuous earthquake activity monitoring. On the other hand, seismic risk
39 management requires consequence-based measures of the earthquake potential. Indeed, loss
40 forecasting allows cost/benefit analysis to compare different options for risk mitigation and then to
41 optimally allocate resources. In fact, given a set of possible risk mitigation actions $\{A_1, A_2, \dots, A_i, \dots, A_n\}$,
42 which includes the option of no-action, and the expected value of the loss associated to each of them
43 $\{E[L|A_1], E[L|A_2], \dots, E[L|A_i], \dots, E[L|A_n]\}$, which includes the cost to undertake the action, a
44 criterion for the optional decision (D) is to undertake the action $A^* \in \{A_1, A_2, \dots, A_n\}$ such that the
45 estimated expected loss is minimized (Benjamin and Cornell, 1970); Equation (1).

$$46 \quad D(A^*) \text{ is optimal} \stackrel{\text{def}}{\Leftrightarrow} E[L|A^*] \leq E[L|A_i] \quad \forall i = 0, 1, \dots, n. \quad (1)$$

47 On these premises, the present study discusses, focusing on the Italian case, the feasibility of
48 probabilistic seismic loss assessment, when seismicity rates based on OEF represent the input. For
49 Italy, these rates are continuously provided by an experimental OEF system (see Marzocchi et al.,
50 2014, and references therein for discussions about the use of OEF models during seismic swarms).

51 The OEF output provides the basis for a short-term adaption of probabilistic seismic hazard
52 analysis (PSHA; e.g., McGuire, 2004). Indeed, short-term PSHA may be derived from OEF rates if the
53 probability to observe a given macroseismic (MS) intensity level in one earthquake, or alternatively, to
54 exceed a ground motion intensity measure (IM) threshold, is available (to follow). In fact, the risk
55 assessment also needs models for the vulnerability of the built environment conditional to any
56 earthquake intensity level. Finally, probabilistic measures of loss (e.g., casualties) conditional to
57 damage, that is exposure models, are also required.

58 Starting from these risk components, a procedure was set-up to compute a number of site-specific
59 and regional (i.e., referring to a number of sites in the same area) loss measures, consistent with the
60 performance-based earthquake engineering approach (Cornell and Krawinkler, 2000). The risk metrics
61 considered include: damaged or collapsed buildings, displaced residents, injuries and fatalities.

62 The procedure developed, which is virtually independent on the seismological model used to carry
63 out OEF, was coded in a prototypal operational earthquake loss forecasting (OELF) system, namely
64 MANTIS-K, which is currently under experimentation for potential civil protection purposes. The
65 system continuously receives daily input from OEF procedures and carries out OELF for the whole
66 country immediately after each update of seismicity rates. The loss forecasting refers to one week after
67 the OEF data release.

68 Even if, intentionally, the developed study does not present any specific advancement in the
69 seismological and earthquake engineering models employed, which all reflect published
70 methodologies, the developed study is deemed innovative as it represent, to date and to the knowledge
71 of the authors, the first prototype of a, continuously operating, nationwide seismic risk estimation
72 system, virtually enabling real-time risk management.

73 In the following, the stochastic framework developed to pass from OEF-based seismicity rates to
74 short-term loss forecasting is presented first. The illustration of the procedure starts from short-term
75 seismic hazard, expressed in terms of *MS* and *IM*, based on a source cell to which a seismicity rate is
76 assigned by OEF. Then, building damage and casualty rates for a site exposed to multiple source cells
77 in an area (e.g., the area of a seismic swarm) are formalized, and the stochastic hypotheses to pass
78 from the weekly number of casualty-producing events at a site, to regional expected losses in an area
79 of interest, are discussed. Subsequently, regional hazard and risk measures (i.e., those requiring to
80 account for spatial correlation of ground motion) are briefly addressed. The second section describes
81 the exposure and vulnerability models considered, based on national census and empirically-calibrated
82 damage probability matrices (DPM) for Italy, respectively. Finally, to illustrate how the implemented
83 experimental OELF system operates, the 2012 Pollino (southern Italy) sequence, which featured a
84 magnitude 5 event (the largest in the sequence), is analyzed. Four days are taken as representative of
85 the evolution of the swarm, in terms of forecasted seismicity: (i) before the swarm, (ii) during the

86 swarm just before the largest magnitude earthquake, (iii) during the swarm after the largest magnitude
87 event, and (iv) post-swarm. At each of the four instants the expected losses, in one-week time-horizon,
88 are computed for an area within 70 km from a point identified as the center of the swarm. A
89 comparison of the loss assessment carried out based on OEF with the one computed using, for the
90 same area, the seismicity rates used for the long term hazard mapping of the country, is also shown.

91 **Methodology**

92 Given a region monitored by a seismic sensor network, OEF models may provide, for each elementary
93 area in which the territory is divided and identified by a pair of coordinates $\{x, y\}$, the estimated
94 expected number of earthquakes above a magnitude of interest per unit time (for example one week).
95 Such a rate, $\lambda(t, x, y | H(t))$, depends on the recorded seismicity history, $H(t)$, and consequently
96 varies with time, t . In this context, if the grid is sufficiently small, the point of coordinates $\{x, y\}$ may
97 be treated as a point-like seismic source; i.e., the centroid of a cell representing an elementary seismic
98 source zone.

99 Considering a site of coordinates $\{w, z\}$, in which there is exposure to seismic risk, for example
100 one or more residential buildings, it is possible to transform the rate above into the expected number of
101 events that, at the $\{w, z\}$ location, will cause the occurrence of certain MS level, or exceedance of an
102 IM threshold. In the following equations are written in terms of MS , yet an equivalent procedure can
103 be set up in terms of IM , as illustrated in the subsequent section.

104 The sought rate for an arbitrary macroseismic intensity level, ms , that is $\lambda_{MS=ms}(t, w, z | H(t))$, is
105 obtained filtering $\lambda(t, x, y | H(t))$, that is multiplying it by the probability that an earthquake
106 generated in $\{x, y\}$, with known distance from $\{w, z\}$, $R(x, y, w, z)$, causes the considered effect in
107 terms of MS , $P[MS = ms | R(x, y, w, z)]$; Equation (2).

108
$$\begin{aligned} \lambda_{MS=ms}(t, w, z | H(t)) &= \lambda(t, x, y | H(t)) \cdot P[MS = ms | R(x, y, w, z)] = \\ &= \lambda(t, x, y | H(t)) \cdot \int_m P[MS = ms | m, R(x, y, w, z)] \cdot f_M(m) \cdot dm \end{aligned} \quad (2)$$

109 In the equation $P[MS = ms | m, R(x, y, w, z)]$ is the probability of observing ms at $\{w, z\}$ given an
 110 earthquake of magnitude m at $\{x, y\}$, and emphasizes that attenuation models (i.e., prediction
 111 equations) providing such probabilities are dependent not only on the distance, but also (at least) on a
 112 random variable (RV) accounting for the earthquake intensity at the source; e.g., the earthquake
 113 magnitude, M . Indeed, $f_M(m)$ is the magnitude distribution of earthquakes at the $\{x, y\}$ seismic
 114 source. (Some models for MS use an equivalent of magnitude instead; it is called the expected
 115 intensity at the epicenter or I_E ; e.g., Pasolini et al., 2008.)

116 If the $\{w, z\}$ site is subjected to several point sources, the total rate is given in Equation (3), as the
 117 summation of terms in Equation (2) over the source area. This equation is not different from a
 118 classical seismic hazard integral, except that the rate of events is time-variant, which is not the
 119 common assumption in PSHA.

120
$$\lambda_{MS=ms}(t, w, z | H(t)) = \int_x \int_y \lambda(t, x, y | H(t)) \cdot \int_m P[MS = ms | m, R(x, y, w, z)] \cdot f_M(m) \cdot dm \cdot dy \cdot dx \quad (3)$$

121 An extension of Equation (3), including a vulnerability term, allows to compute the rate of events
 122 causing some damage state (ds) to a building of a given structural typology (k). This is given in
 123 Equation (4), where $P[DS^{(k)} = ds | ms]$ is the damage probability for the structural typology of interest
 124 given ms ; i.e., a DPM (to follow).

125
$$\begin{aligned} \lambda_{DS^{(k)}=ds}(t, w, z | H(t)) &= \int_x \int_y \lambda(t, x, y | H(t)) \cdot \\ &\sum_{ms} P[DS^{(k)} = ds | ms] \cdot \int_m P[MS = ms | m, R(x, y, w, z)] \cdot f_M(m) \cdot dm \cdot dy \cdot dx \end{aligned} \quad (4)$$

126 Even if it was just mentioned that these rates may not be constant over wide time intervals, such a
 127 hypothesis may be acceptable in the short-term (for example unless an update of seismicity from OEF
 128 is available). Thus, in the (small) time interval $(t, t + \Delta t)$, the probability of observing one event

129 producing a damage state equal to ds to a building of the structural typology k , can be computed
 130 through Equation (5). This equation assumes that the stochastic process of events causing damage to
 131 the building at the site is locally (in time) approximated by a (homogeneous) Poisson process. (Note
 132 that dependence on $\{w, z\}$ at the left hand side is dropped for simplicity in this equation and in those
 133 derived from it.)

$$134 \quad P\left[DS_{(t,t+\Delta t)}^{(k)} = ds | H(t)\right] \approx \lambda_{DS^{(k)}=ds}(t, w, z | H(t)) \cdot \Delta t \quad (5)$$

135 If number of buildings of the k -th structural typology, $N_B^{(k)}$, is known for the $\{w, z\}$ site (i.e., a
 136 measure of the exposure), then the expected number of buildings in damage state ds in $(t, t + \Delta t)$ can
 137 be computed via Equation (6). It is worth noting that cumulated damages due to subsequent events,
 138 which can eventually lead to building failure, are neglected, even if this issue can virtually be
 139 accounted for in the considered methodology.

$$140 \quad E\left[N_{ds,(t,t+\Delta t)}^{(k)} | H(t)\right] = N_B^{(k)} \cdot P\left[DS_{(t,t+\Delta t)}^{(k)} = ds | H(t)\right] \quad (6)$$

141 In fact, Equation (4) may be further extended in the direction of earthquake consequences if for the k -
 142 th structural typology, and conditional to damage, the probability of an occupant to suffer casualties,
 143 $P\left[Cas^{(k)} | ds\right]$, is available. Then, it is possible to compute the rate of events producing the considered
 144 loss, $\lambda_{Cas^{(k)}}(t, w, z | H(t))$, as in Equation (7).

$$145 \quad \lambda_{Cas^{(k)}}(t, w, z | H(t)) = \int \int_{x \ y} \lambda(t, x, y | H(t)) \cdot \sum_{ds} P\left[Cas^{(k)} | ds\right] \cdot \sum_{ms} P\left[DS^{(k)} = ds | ms\right] \cdot \int_m P\left[MS = ms | m, R(x, y, w, z)\right] \cdot f_M(m) \cdot dm \cdot dx \cdot dy \quad (7)$$

146 The latter equation, formally equivalent to the PBEE framing equation (Cornell and Krawinkler,
 147 2000), is the one of interest and it provides the rate of events producing casualties (e.g., fatality, injury,
 148 or shelter need) for an occupant of a building of the k -th typology at the $\{w, z\}$ site. It also allows to
 149 compute of expected values of ultimate earthquake consequences because, in the same hypotheses of
 150 Equation (5), the probability of observing an event determining casualties, $P\left[Cas_{(t,t+\Delta t)}^{(k)} | H(t)\right]$, may
 151 be obtained via Equation (8). Then, the expected number of casualties in the time interval of interest,

152 $E\left[N_{Cas,(t,t+\Delta t)}^{(k)}|H(t)\right]$, can be computed through Equation (9), if the number of residents, $N_p^{(k)}$, in
 153 buildings of the k -th typology at $\{w, z\}$ is available.

$$154 \quad P\left[Cas_{(t,t+\Delta t)}^{(k)}|H(t)\right] \approx \lambda_{Cas^{(k)}}(t, w, z|H(t)) \cdot \Delta t \quad (8)$$

$$155 \quad E\left[N_{Cas,(t,t+\Delta t)}^{(k)}|H(t)\right] = N_p^{(k)} \cdot P\left[Cas_{(t,t+\Delta t)}^{(k)}|H(t)\right] \quad (9)$$

156 Note that the expected losses as per Equation (6) and Equation (9) may be considered as site-specific
 157 risk measures; however, it is probabilistically rigorous to sum them up over all the exposed sites of
 158 interest to compute the expected number of casualties in the area (see also the application section).

159 **Site-specific and regional risk assessment based on ground motion intensity**

160 In the same underlying hypotheses of Equation (3), it is possible to compute the average number per
 161 unit-time of events, $\lambda_{IM>im}$, that cause the exceedance of an IM threshold, im , at the $\{w, z\}$ site. Such
 162 a rate is given in Equation (10), where the $P[IM > im | m, R(x, y, w, z)]$ term is from a ground motion
 163 prediction equation, or GMPE (e.g., Ambraseys et al., 1996). (Note that, GMPEs, differently from
 164 macroseismic intensity prediction equations, require geological information about the $\{w, z\}$ site.)

$$165 \quad \begin{aligned} \lambda_{IM>im}(t, w, z | H(t)) = \\ = \int_x \int_y \lambda(t, x, y | H(t)) \cdot \int_m P[IM > im | m, R(x, y, w, z)] \cdot f_M(m) \cdot dm \cdot dx \cdot dy \end{aligned} \quad (10)$$

166 Consequent to Equation (10), the rate of events causing some $DS = ds$ to a building of typology k ,
 167 may be computed via Equation (11), where the term $P[DS^{(k)} = ds | im]$ is the fragility curve for the
 168 building (note that one fragility is required for each DS level).

$$169 \quad \begin{aligned} \lambda_{DS^{(k)}=ds}(t, w, z | H(t)) = \int_x \int_y \lambda(t, x, y | H(t)) \cdot \\ \int_{im} P[DS^{(k)} = ds | im] \cdot \int_m f_{IM|M,R}(im, R(x, y, w, z)) \cdot f_M(m) \cdot dm \cdot d(im) \cdot dy \cdot dx \end{aligned} \quad (11)$$

170 It is also possible to use the IM-based rates in Equation (10) to compute $\lambda_{DS^{(k)}=ds}$ employing DPMs in
 171 terms of macroseismic intensity; i.e., Equation (12). Of course this requires a probabilistic relationship

172 (e.g., a semi-empirical model) between IM and MS , that is the $P[MS = ms|im]$ term. This kind of
 173 models exists, also calibrated on Italian data; e.g., Faenza and Michelini (2010).

$$\begin{aligned}
 \lambda_{DS^{(k)}=ds}(t, w, z|H(t)) &= \int_x \int_y \lambda(t, x, y|H(t)) \cdot \\
 \sum_{ms} P[DS^{(k)} = ds|ms] &\cdot \int_{im} P[MS = ms|im] \cdot \int_m f_{IM|M,R}(im, R(x, y, w, z)) \cdot f_M(m) \cdot dm \cdot d(im) \cdot dy \cdot dx
 \end{aligned} \tag{12}$$

175 Along the same line, the rate of events causing casualty, may be computed in Equation (13), with
 176 obvious meaning of the symbols. At this point these rates can be used to compute the individual risk
 177 metrics in Equation (8) and Equation (9). Note that in principle, this should lead to the same results as
 178 if the expected losses are computed using MS as the hazard-related measure, even if, because of the
 179 semi-empirical models used in both approaches, differences may be expected.

$$\begin{aligned}
 \lambda_{Cas^{(k)}}(t, w, z|H(t)) &= \int_x \int_y \lambda(t, x, y|H(t)) \cdot \sum_{ds} P[Cas^{(k)}|ds] \cdot \int_{im} P[DS^{(k)} = ds|im] \cdot \\
 \int_m f_{IM|M,R}(im, R(x, y, w, z)) &\cdot f_M(m) \cdot dm \cdot d(im) \cdot dy \cdot dx
 \end{aligned} \tag{13}$$

181 Because the IMs or MS' at different sites in a given earthquake are stochastically dependent, also the
 182 losses (i.e., building damage and casualties) are dependent. Therefore, in general, it not easy to
 183 compute the probability of observing a certain value of the loss over a region (i.e., the distribution of
 184 the total regional loss). Nonetheless, the expected number of damaged buildings, or casualties at each
 185 site, may be summed up over a region of interest to obtain global averages, which justifies equations
 186 derived in the previous section. This is because the expected value is not affected by stochastic
 187 dependency of the added RVs.

188 Conversely, if one wants, for example, to compute the probability that at least one building of the
 189 region will get in some damage state in the forthcoming week, then all the sites have to be treated
 190 jointly. In fact, this issue primarily raises from the hazard, because to compute, for example, the rate of
 191 earthquakes in the region, which will cause exceedance of an IM threshold at least at one of the
 192 $\{1, 2, \dots, i, \dots, n\}$ sites, $\lambda_{\{\exists i: IM_i > im\}}$, Equation (14) is required, which may be referred to as a regional
 193 hazard integral; e.g., Esposito and Iervolino (2011).

194
$$\lambda_{\{\exists i:IM_i>im\}} = \int \int_{x y} \lambda(t, x, y | H(t)) \cdot \left\{ 1 - \int_m P \left[\bigcap_{i=1}^n IM_i \leq im \mid M, \underline{R}(x, y, \underline{w}, \underline{z}) \right] \cdot f_M(m) \cdot dm \right\} \cdot dx \cdot dy \quad (14)$$

195 In the equation the $P \left[\bigcap_{i=1}^n IM_i \leq im \mid M, \underline{R}(x, y, \underline{w}, \underline{z}) \right]$ term is the joint probability of the *IMs* at the *n*
 196 sites (note that in the equation *w* and *z* are vectors in this case). This distribution has to be used to
 197 properly account for intraevent correlation that exists among *IMs* in different sites. This correlation
 198 arises because of two factors: (i) the considered sites share the same event features (i.e., earthquake
 199 magnitude and location); (ii) intraevent residuals of *IMs*, with respect to a GMPE, are (in principle)
 200 spatially correlated (e.g., Esposito and Iervolino, 2012).

201 That said, the rates in Equation (14) may be used to approximate probabilities of interest, in
 202 analogy with Equation (5). For example, the probability of events causing at least one damaged
 203 building (or casualty), or the probability of observing a certain number of damaged buildings (or
 204 casualties), in the region, may be computed. However, this may imply large computational effort due
 205 to the likely required Monte Carlo simulation of random fields of losses at all sites. Indeed, an
 206 individual building location is virtually a site with an associated *IM* random variable. Moreover, it
 207 may also be required to account for spatial correlation of building damage given intensity or of
 208 casualty given damage. This is not discussed here further, as the developed system primarily works in
 209 terms of expected losses.

210 The flowchart in Figure 1 recaps the described procedure to compute the discussed site-specific and
 211 regional short-term risk measures, starting from time-variant seismicity estimations from OEF. The
 212 following section describes the models and data for hazard, vulnerability, and exposure employed for
 213 OELF in Italy.

214 **Models and data for OELF in Italy**

215 **Seismicity rates**

216 Seismicity rates from OEF, $\lambda(t, x, y | H(t))$, are provided by the OEF-Italy system of the (Italian)
217 national institute of geophysics and volcanology (INGV) for a grid spaced of about 0.1° and covering
218 the whole national area and some sea. They are obtained based on the seismicity recorded by the
219 country-wide seismic network of INGV and are updated daily or after a $M 3.5+$ (local magnitude scale
220 is used) event in the monitored area. The time unit for rates is one week and they refer to events with
221 local magnitude equal or larger than four (Marzocchi et al., 2014). The magnitude of these events is
222 supposed, herein, to be distributed according to a Gutenberg-Richter-type relationship (Gutenberg and
223 Richter, 1994), with unbounded maximum magnitude and b -value equal to one. This relationship does
224 not change with the point source a specific rate value refers to; i.e., it is spatially-invariant.

225 It is not the focus of this work to scientifically discuss OEF models, and it has to be underlined that
226 the risk assessment procedure is practically independent of how input data (i.e., seismicity rates for
227 point-like cells discretizing the territory) are computed; therefore, the reader is referred to Marzocchi
228 et al (2014) for further details.

229 **Earthquake intensity**

230 The chosen prediction equation for macroseismic intensity is that of Pasolini et al. (2008), which is
231 also adopted by INGV for the assessment of macroseismic national hazard (Gómez Capera et al.,
232 2007). Intensity is defined by the Mercalli-Cancani-Sieberg (MCS) scale (Sieberg, 1931) and the
233 explanatory variables of the model are epicentral distance, R_{epi} , and I_E (epicentral intensity). The
234 model applies to the [0km,220km] interval of the former, and between 5 and 12 of the latter. (Cardinal
235 numbers are used for MS, in lieu of ordinals, consistent with the cited study.)

236 Pasolini et al. (2008) also provide a semi-empirical model relating epicentral intensity, I_E , and the
237 moment magnitude, M_w , from which the distribution of epicentral intensity conditional to moment
238 magnitude, $f_{I_E|M_w}(i_E|m)$, may be obtained. Thus for each point source, the I_E distribution, $f_{I_E}(i_E)$,

239 may be obtained through the marginalization in Equation (15). These distributions are conditional to
 240 the earthquake occurrence at the specific point-like source.

$$241 \quad f_{I_E}(i_E) = \int_m f_{I_E|M_w}(i_E|m) \cdot f_{M_w}(m) \cdot dm \quad (15)$$

242 According to the adopted model for *MS* attenuation, in the equations above the I_E RV and its
 243 distribution, $f_{I_E}(i_E)$, have to replace M and $f_M(m)$, respectively.

244 In the loss assessment, contributions from sources with epicentral distance larger than 150km are
 245 neglected. Moreover, in order to convert the continuous model of *MS* provided by Pasolini et al.
 246 (2008) into a discrete model, mass probabilities associated to integer values of *ms* between 0 and 12
 247 are computed. Then, conditional to the occurrence of the earthquake, the resulting *ms* distribution for
 248 each site is scaled such that $P[0 \leq ms \leq 12] = 1$. It is to finally note that the considered model applies
 249 for M_w up to about 7; therefore, the magnitude distribution of the sources has been truncated to $M_w \leq 7$;
 250 consequences of such an assumption were verified for tolerability. The check was carried out
 251 considering, in the loss assessment, magnitudes up to ten and extrapolating the models up to this
 252 magnitude. It was verified that the weekly expected losses did change (in the worst case) in the order
 253 of 10% with respect to the truncation to magnitude seven.

254 **Vulnerability**

255 For each vulnerability class (k) and conditional to *MS*, models of structural vulnerability provide the
 256 $P[DS^{(k)} = ds | ms]$ terms, which are usually computed based on empirical data. These probabilities are
 257 traditionally arranged in the form of a matrix with the number of rows equal to number of structural
 258 classes considered times the possible *MS* intensities, whereas the number of columns is the number of
 259 considered damage states. The resulting matrix is referred to as a damage probability matrix.

260 The DPM considered in this study (Iervolino et al, 2014) is based on Italian observational data
 261 (Zuccaro and Cacace, 2009). The DPM, reported in Table 1, accounts for four different vulnerability
 262 classes from A to D, and six damage levels ($D0$ – no damage, $D1$ – slight damage, $D2$ – moderate
 263 damage, $D3$ – heavy damage, $D4$ – very heavy damage, $D5$ collapse). Vulnerability classes, damage

264 levels and MS are defined in accordance with the European macroseismic scale or EMS 98 (Grünthal,
265 1998). In fact, in this paper, DPM are applied to the hazard assessment in term of MCS. Moreover it is
266 worth to note that, due to the lack of Italian observational data, DPM values for $MS \geq 11$ are based on
267 extrapolation.

268 Casualty probabilities conditional to a given structural damage and vulnerability class,
269 $P[Cas^{(k)}|ds]$, are those of Zuccaro and Cacace (2011), in which fatalities and injuries are considered
270 (someone requiring hospital treatment is defined as injured); Table 2. Zero probability is associated to
271 damage levels equal to or lower than $D3$, whereas for $D4$ and $D5$ casualty probabilities are provided
272 for each vulnerability class from A to D. The probability of being displaced for a resident in a building
273 in damage level $D4$ or $D5$ is one, while is 0.5 for buildings in $D3$, and zero for lower damage levels.

274 **Exposure**

275 For exposure, municipalities are the elementary units in which the Italian territory is divided. Data
276 regarding the number of buildings and the number of residents (both grouped by vulnerability class)
277 are derived from the National census of 2001 (Zuccaro et al., 2012).

278 According to Zuccaro et al. (2012), casualty and injury assessment may be carried out considering
279 that 65% of the total population is exposed at the time of occurrence of the earthquake, that is the term
280 $N_p^{(k)}$ in Equation (9) is multiplied by 0.65. (In fact, Zuccaro and Cacace (2011) provide hourly
281 occupancy ratios, which are, however, neglected herein.)

282 **The MANTIS-K system and an illustrative application**

283 The described procedure and data have been implemented in an automatic system, currently under
284 experimentation that receives the output of the OEF-Italy system in real-time. The system computes,
285 in about 1.5 hours on a today's ordinary personal computer, for each vulnerability class, on a
286 municipality basis, the probabilities that in one week after the OEF release:

- 287 - a building becomes unusable for seismic causes;
- 288 - a building collapses for seismic causes;

289 - the occupant of a building is injured for seismic causes;

290 - the occupant of a building dies for seismic causes.

291 As an example, panels a-d of Figure 2 report the countrywide probability of collapse of buildings given
292 the vulnerability class in the week after October 26th 2012. In the same week, panels a-d of Figure 3
293 report the probability of a generic building to collapse, as well as of being unusable. The figure also
294 reports the injury and fatality probability for the whole country. Actually, for an arbitrary area in the
295 country, MANTIS-K can compute the weekly total expected number of:

296 - collapsed buildings;

297 - displaced residents;

298 - injuries;

299 - fatalities.

300 In fact, the system, at each release of the OEF rates, automatically identifies the location in Italy for
301 which the rate from the OEF-Italy system is the largest. For an area of 140 km in diameter around this
302 point, which is defined as the one with the largest current seismicity, the system computes the
303 expected losses in terms of total expected number of collapsed buildings, displaced residents, injuries
304 and fatalities. This should automatically provide the risk for the most hazardous area according to the
305 current OEF estimate (as also illustrated in the next subsection).

306 The discussed risk metrics are expressed in terms of probabilities for the week after the release of
307 OEF rates primarily because the OEF-Italy system of INGV releases weekly rates; however, it also
308 believed that one week is a time-span sufficient also to put in place risk reduction actions, if needed;
309 therefore this time-frame was kept for the loss assessment. It is also to note that, because the OEF rates
310 are released by INGV at least daily, the weekly probabilities are updated at each OEF rates release;
311 therefore, at least daily as well.

312 In principle, the losses computed via this system can be compared, in the framework of Equation
313 (1), to the expected losses in the case some risk reduction action is hypothetically put in place in a
314 region affected by a seismic swarm. This may aid decision making with respect to taking the decision
315 which minimizes the expected loss.

316 **The 2012 Pollino sequence**

317 In this section OELF is applied to the Pollino (southern Italy) seismic sequence, which lasted several
318 months and featured a M_w 5 event in October 2012, which was the largest magnitude observed. Four
319 OEF outputs are here considered for the risk assessment, they are based on OEF rates released at 00:00
320 (UTC) of the following days: (a) 01/01/2010; (b) 25/10/2012; (c) 26/10/2012; (d) 21/07/2013. Release
321 (a) is considered representative of conditions before the start of the seismic sequence, whereas (b) and
322 (c) are before and after the largest magnitude event, respectively. Finally, (d) is several months after
323 the largest magnitude event.

324 For each of these instants, INGV provided $\lambda(t, x, y | H(t))$ for the whole national area. From these
325 rates, represented in panels a-d of Figure 4, it can be noted that only on 10/26/2012 the Pollino area is
326 the most hazardous in Italy (that is right after the largest magnitude event; this is a specific feature of
327 the OEF models used as an input herein). More specifically, maximum values of seismicity is at the
328 grid point of coordinates lat. 39.85° and long. 16.05° , which is hereafter identified as the center of the
329 Pollino sequence. The expected number of $M_w \geq 4$ events in the week following instant (c) is equal
330 to 0.0615000 [events/week]. Rates estimated by INGV at the same point for instants (a), (b), and (d),
331 are 0.0000727 [events/week], 0.002260 [events/week], and 0.000672 [events/week], respectively. For
332 the risk assessment, all municipalities within a radius of 70 km from the center of the sequence are
333 considered; in Figure 5 these municipality are plotted with a color-scale reflecting the expected
334 number of fatalities in the week after 26/10/2012.

335 The centroid of each municipality area is considered for computing the distance from each point-
336 like seismic source, $R(x, y, w, z)$, which is required by the attenuation model. Clearly, there are two
337 implicit assumptions behind this choice: the first is that it is possible to concentrate in a single point
338 the whole vulnerability and exposure of each municipality; the second is that such a point is the
339 geometrical center of each municipality.

340 Applying Equation (6) and Equation (9), the expected number of: (i) collapsed buildings (i.e.,
341 buildings damage levels $D4$ and $D5$), (ii) displaced, (iii) injured, and (iv) dead residents, in the week
342 following each of the four considered instants was computed for each municipality. In Table 3, results

343 are summed up per bin of distance from the center of the Pollino area. In the same table, risk indices
344 are normalized with respect to the total number of buildings or residents in each distance bin.

345 These results allow to point out that risk measures are sensitive to the short-term seismicity
346 variations inferred by OEF. On the other hand, if absolute values of indices are considered, the largest
347 computed risk (at time 3) is about one expected fatality over more than $4 \cdot 10^5$ residents within a radius
348 of 50 km from the center of the sequence (note that, according to the information available to the
349 authors, no casualties were recorded in the Pollino sequence).

350 The largest evaluated risk is just after the largest shock observed. This feature stems from the OEF
351 models used in the OEF-Italy system, which yield an expected seismicity rate that is proportional to
352 the seismic moment already released.

353 **Comparison with losses based on long-term hazard**

354 Further insights regarding from these results may be obtained by comparing them with the weekly loss
355 computed using the seismic source model of Meletti et al. (2008), with rates from Barani et al. (2009),
356 which lie at the basis of the national hazard map for Italy (Stucchi et al., 2011), used for structural
357 design. This model considers areal source zones and no background seismicity. The rates associated to
358 each source zone are annual and were scaled to one week, for the purposes of this study, using a $7/365$
359 conversion factor. Because the Barani et al. (2009) study provides rates for earthquakes with minimum
360 magnitude equal to 4.3 (for all zones, but zone named 936, which is has a minimum magnitude of 3.7),
361 these rates have been adjusted herein to include earthquakes with magnitude between 4 and 4.3. This
362 was to be consistent with the minimum magnitude from the OEF-Italy system, and such an adjustment
363 was carried out via a Gutenberg-Richter relationship with a b -value equal to one. The resulting rates
364 for Italy are given in Figure 6 along with the seismic source zones.

365 Weekly expected losses with this source model were computed for the Pollino area. In risk
366 analysis, except of the rates, all others models and assumptions being the same as those based on OEF;
367 i.e., those discussed above. Results, are reported in Table 4, which shows a good agreement with those
368 computed for day (a) and day (d) of the Pollino sequence. This was somewhat expected as (a) and (d)
369 were identified as a pre-swarm and post-swarm instants, and therefore the risk associated to them

370 should grossly reconcile (i.e., same order of magnitude) with loss assessment based on long-term
371 hazard. To better understand this comparison of losses based on OEF with respect to those from the
372 assessment based on long-term seismicity rates, Table 5 reports the ratios of the losses computed
373 during the Pollino sequence (Table 3) divided by those of Table 4.

374 **Conclusions**

375 The study discussed, focusing on the Italian case, the feasibility of probabilistic short-term seismic
376 loss (risk) assessment, when the input is represented by the seismicity rates given by the operational
377 earthquake forecasting procedures.

378 Given data available in terms of vulnerability and exposure for Italy, and the seismicity data
379 provided daily by the OEF-Italy system of the Italian national institute of geophysics and volcanology,
380 an experimental system for continuous nationwide short-term seismic risk assessment, MANTIS-K,
381 was set-up. According to the output of OEF, the forecasted consequence statistics are for one-week
382 time-horizon after the time of the analysis. Risk metrics are the expected number of collapsed
383 buildings, fatalities, injuries, and displaced residents. In fact, an illustrative application, which does
384 not discuss the scientific merit of input seismicity data and vulnerability/exposure models employed,
385 was developed. It refers to the 2012 Pollino (southern Italy) sequence.

386 The main conclusions from this feasibility study are that: (i) probabilistically-consistent continuous
387 short-term seismic risk assessment in Italy appears to be feasible; (ii) the approach is probabilistically
388 rigorous and it is virtually independent of the OEF and vulnerability/exposure models employed, while
389 results, obviously, are not; (iii) the risk measures considered seem to be sensitive to the short-term
390 seismicity variations inferred by OEF, that is, orders of magnitude variations of seismicity rates are
391 reflected in orders of magnitude variations of casualty rates; (iv) because of the intrinsic feature of the
392 OEF model employed, the largest risk is observed after the largest-magnitude event observed in the
393 sequence, indicating the moment in which a worse earthquake is more likely.

394 **Data and resources**

395 OEF rates from the OEF-Italy system of INGV were provided by Warner Marzocchi. Damage
396 probability matrices and exposure information were provided by Giulio Zuccaro. The rest of data is
397 from the listed references.

398 **Acknowledgements**

399 The study presented in this paper was developed partially within the activities of Rete dei Laboratori
400 Universitari di Ingegneria Sismica (ReLUIS) for the research program funded by the Dipartimento
401 della Protezione Civile (2014-2018), and partially in the framework of AMRA – Analisi e
402 Monitoraggio dei Rischi Ambientali scarl for the strategies and tools for real-time earthquake
403 risk reduction (REAKT) funded by the European Community via the Seventh Framework Program for
404 Research, with contracts no. 282862. Ned Field, the associate editor of BSSA, Martin C. Chapman,
405 and an anonymous reviewer, whose comments helped to improve quality and readability of this paper
406 are also acknowledged.

407 **References**

- 408 Ambraseys, N. N, K. A. Simpson and J. J. Bommer (1996). Prediction of horizontal response spectra
409 in Europe, *Earthquake Engineering and Structural Dynamics* **25** 371–400.
- 410 Barani, S., D. Spallarossa, and P. Bazzurro (2009). Disaggregation of probabilistic ground-motion
411 hazard in Italy, *B. Seismol. Soc. Am.* **99** 2638-2661.
- 412 Benjamin, J. R., and C. A. Cornell (1970). *Probability, statistics, and decision for civil engineers*,
413 McGraw-Hill, New York.
- 414 Cornell, C. A., and H. Krawinkler (2000). *Progress and challenges in seismic performance*
415 *assessment, PEER Center News* **3** 1-3.
- 416 Esposito, S., and I. Iervolino (2011). PGA and PGV spatial correlation models based on European
417 multi-event datasets, *B. Seismol. Soc. Am.* **101** 2532–2541.

418 Esposito, S., and I. Iervolino (2012). Spatial correlation of spectral acceleration in European data, *B.*
419 *Seismol. Soc. Am.* **102** 2781-2788.

420 Gómez Capera, A.A., C. Meletti, A. Rebez, and M. Stucchi (2007). *Mappa di pericolosità sismica in*
421 *termini di intensità macrosismica ottenuta utilizzando lo stesso impianto metodologico di MPS04,*
422 *Convenzione INGV-DPC 2004-2006/Progetto S1, Deliverable D7. (In Italian.)*

423 Grünthal, G. (Ed.) (1998). *European Macroseismic Scale 1998*, Centre Européen de Géodynamique et
424 Séismologie, Cahiers du Centre Européen de Géodynamique et de Séismologie, Luxemburg.

425 Gutenberg, B., and C. F. Richter (1944). Frequency of earthquakes in California, *B. Seismol. Soc.*
426 *Am.* **34** 185-188.

427 Iervolino, I., E. Chioccarelli, M. Giorgio, W. Marzocchi, A. M. Lombardi, G. Zuccaro, and F. Cacace
428 (2014). Operational earthquake loss forecasting in Italy: preliminary results. Proc. of *Second*
429 *European Conference on Earthquake Engineering and Seismology*, Istanbul, Turkey.

430 Jordan, T. H., Y.- T. Chen, P. Gasparini, R. Madariaga, I. Main, W. Marzocchi, G. Papadopoulos, G.
431 Sobolev, K. Yamaoka, and J. Zschau (2011). Operational Earthquake Forecasting: State of
432 Knowledge and Guidelines for Utilizations, *Ann. Geophys.-Italy* **54** 319-391

433 Marzocchi, W., A. M. Lombardi, and E. Casarotti (2014). The establishment of an operational
434 earthquake forecasting system in Italy, *Seismol. Res. Lett.* **85** 961-969.

435 McGuire, R. K. (2004). *Seismic Hazard and Risk Analysis*, Earthquake Engineering Research Institute
436 Publication, Oakland, CA.

437 Meletti, C., F. Galadini, G. Valensise, M. Stucchi, R. Basili, S. Barba, et al. (2008). A seismic source
438 zone model for the seismic hazard assessment of the Italian territory. *Tectonophysics* **450** 85-
439 108.

440 Faenza, L., and A. Michelini (2010). Regression analysis of MCS intensity and ground motion
441 parameters in Italy and its application in ShakeMap, *Geoph. J. Int.* **180** 1138-1152.

442 Pasolini, C., D. Albarello, P. Gasperini, V. D'Amico, and B. Lolli (2008). The attenuation of seismic
443 intensity in Italy, Part II: Modelling and Validation, *B. Seismol. Soc. Am.* **98** 692-708.

- 444 Sieberg, A. (1931). Erbeben, in Handbuch der Geophysik, B. Gutenberg (Editor), **4** 552–554. (*In*
445 *German.*)
- 446 Stucchi, M., C. Meletti, V. Montaldo, H. Crowley, G. M. Calvi, and E. Boschi (2011). Seismic hazard
447 assessment (2003–2009) for the Italian building code, *B. Seismol. Soc. Am.* **101** 1885-1911.
- 448 Zuccaro, G., and F. Cacace (2009). Revisione dell’inventario a scala nazionale delle classi tipologiche
449 di vulnerabilità ed aggiornamento delle mappe nazionali di rischio sismico, Proc. of *XIII*
450 *Convegno l’Ingegneria Sismica in Italia*, ANIDIS, Bologna, Italy. (*In Italian.*)
- 451 Zuccaro G., and F. Cacace (2011). Seismic casualty evaluation: the Italian model, an application to the
452 L’Aquila 2009 event, In *Human Casualties in Earthquakes: progress in modelling and*
453 *mitigation*, R. Spence, E. So, and C. Scawthorn (Editors), Springer, London, UK.
- 454 Zuccaro, G., F. Cacace, and D. De Gregorio (2012). Buildings inventory for seismic vulnerability
455 assessment on the basis of Census data at national and regional scale, Proc. of *15th World*
456 *Conference on Earthquake Engineering*, Lisbon, Portugal.

Table 1. Considered damage probability matrix.

Class	MS	$P[D0 ms]$	$P[D1 ms]$	$P[D2 ms]$	$P[D3 ms]$	$P[D4 ms]$	$P[D5 ms]$
A	5	0.3487	0.4089	0.1919	0.0450	0.0053	0.0002
B	5	0.5277	0.3598	0.0981	0.0134	0.0009	0.0000
C	5	0.6591	0.2866	0.0498	0.0043	0.0002	0.0000
D	5	0.8587	0.1328	0.0082	0.0003	0.0000	0.0000
A	6	0.2887	0.4072	0.2297	0.0648	0.0091	0.0005
B	6	0.4437	0.3915	0.1382	0.0244	0.0022	0.0001
C	6	0.5905	0.3281	0.0729	0.0081	0.0005	0.0000
D	6	0.7738	0.2036	0.0214	0.0011	0.0000	0.0000
A	7	0.1935	0.3762	0.2926	0.1138	0.0221	0.0017
B	7	0.3487	0.4089	0.1919	0.0450	0.0053	0.0002
C	7	0.5277	0.3598	0.0981	0.0134	0.0009	0.0000
D	7	0.6591	0.2866	0.0498	0.0043	0.0002	0.0000
A	8	0.0656	0.2376	0.3442	0.2492	0.0902	0.0131
B	8	0.2219	0.3898	0.2739	0.0962	0.0169	0.0012
C	8	0.4182	0.3983	0.1517	0.0289	0.0028	0.0001
D	8	0.5584	0.3451	0.0853	0.0105	0.0007	0.0000
A	9	0.0102	0.0768	0.2304	0.3456	0.2592	0.0778
B	9	0.1074	0.3020	0.3397	0.1911	0.0537	0.0060
C	9	0.3077	0.4090	0.2174	0.0578	0.0077	0.0004
D	9	0.4437	0.3915	0.1382	0.0244	0.0022	0.0001
A	10	0.0017	0.0221	0.1138	0.2926	0.3762	0.1935
B	10	0.0313	0.1563	0.3125	0.3125	0.1563	0.0313
C	10	0.2219	0.3898	0.2739	0.0962	0.0169	0.0012
D	10	0.2887	0.4072	0.2297	0.0648	0.0091	0.0005
A	11	0.0002	0.0043	0.0392	0.1786	0.4069	0.3707
B	11	0.0024	0.0284	0.1323	0.3087	0.3602	0.1681
C	11	0.0380	0.1755	0.3240	0.2990	0.1380	0.0255
D	11	0.0459	0.1956	0.3332	0.2838	0.1209	0.0206
A	12	0.0000	0.0000	0.0000	0.0010	0.0480	0.9510
B	12	0.0000	0.0000	0.0006	0.0142	0.1699	0.8154
C	12	0.0000	0.0001	0.0019	0.0299	0.2342	0.7339
D	12	0.0000	0.0002	0.0043	0.0498	0.2866	0.6591

459

Table 2. Casualty probabilities conditional structural damage and structural typology.

Loss	Vulnerability Class	<i>D0</i>	<i>D1</i>	<i>D2</i>	<i>D3</i>	<i>D4</i>	<i>D5</i>
Fatality	A or B or C	0	0	0	0	0.04	0.15
Fatality	D	0	0	0	0	0.08	0.3
Injury	A or B or C	0	0	0	0	0.14	0.7
Injury	D	0	0	0	0	0.12	0.5

460

Table 3. Indices of seismic risk across the swarm.

	Dist.	Total build.	Total res.	Coll.	Disp.	Injuries	Fatalities	Coll. [%]	Disp. [%]	Injuries [%]	Fatalities [%]
01/01/2010	≤ 10km	4281	12567	2.85E-02	2.92E-01	1.16E-02	3.00E-03	6.65E-04	2.32E-03	9.25E-05	2.39E-05
	≤ 30km	66243	188538	2.34E-01	2.74E+00	1.03E-01	2.69E-02	3.53E-04	1.45E-03	5.45E-05	1.43E-05
	≤ 50km	149733	438990	5.21E-01	6.14E+00	2.29E-01	5.98E-02	3.48E-04	1.40E-03	5.21E-05	1.36E-05
	≤ 70km	256281	878432	9.07E-01	1.16E+01	4.35E-01	1.14E-01	3.54E-04	1.32E-03	4.96E-05	1.30E-05
25/10/2012	Dist.	Total build.	Total res.	Coll.	Disp.	Injuries	Fatalities	Coll. [%]	Disp. [%]	Injuries [%]	Fatalities [%]
	≤ 10km	4281	12567	1.22E-01	1.05E+00	5.64E-02	1.43E-02	2.85E-03	8.35E-03	4.49E-04	1.14E-04
	≤ 30km	66243	188538	6.17E-01	6.43E+00	2.81E-01	7.27E-02	9.32E-04	3.41E-03	1.49E-04	3.86E-05
	≤ 50km	149733	438990	1.07E+00	1.17E+01	4.77E-01	1.24E-01	7.15E-04	2.66E-03	1.09E-04	2.82E-05
26/10/2012	Dist.	Total build.	Total res.	Coll.	Disp.	Injuries	Fatalities	Coll. [%]	Disp. [%]	Injuries [%]	Fatalities [%]
	≤ 10km	4281	12567	1.87E+00	1.52E+01	8.88E-01	2.24E-01	4.37E-02	1.21E-01	7.06E-03	1.78E-03
	≤ 30km	66243	188538	7.46E+00	7.18E+01	3.47E+00	8.90E-01	1.13E-02	3.81E-02	1.84E-03	4.72E-04
	≤ 50km	149733	438990	1.07E+01	1.08E+02	4.83E+00	1.24E+00	7.13E-03	2.46E-02	1.10E-03	2.84E-04
21/07/2013	Dist.	Total build.	Total res.	Coll.	Disp.	Injuries	Fatalities	Coll. [%]	Disp. [%]	Injuries [%]	Fatalities [%]
	≤ 10km	4281	12567	5.77E-02	5.33E-01	2.54E-02	6.49E-03	1.35E-03	4.24E-03	2.02E-04	5.17E-05
	≤ 30km	66243	188538	3.68E-01	4.06E+00	1.67E-01	4.34E-02	5.55E-04	2.15E-03	8.85E-05	2.30E-05
	≤ 50km	149733	438990	7.27E-01	8.25E+00	3.25E-01	8.47E-02	4.86E-04	1.88E-03	7.39E-05	1.93E-05
≤ 70km	256281	878432	1.17E+00	1.45E+01	5.60E-01	1.47E-01	4.55E-04	1.65E-03	6.37E-05	1.67E-05	

462
463

Dist. means distance; Build. means buildings; Res. means residents; Coll. means collapsed buildings; disp. means displaced residents.

464

Table 4. Indices of seismic risk derived from seismogenic zones and seismic rates from Barani et al. (2009).

Distance	Total buildings	Total residents	Coll.	Disp.	Injuries	Fatalities	Coll. [%]	Disp. [%]	Injuries [%]	Fatalities [%]
≤ 10km	4281	12567	3.74E-02	3.56E-01	1.60E-02	4.09E-03	8.74E-04	2.84E-03	1.27E-04	3.25E-05
≤ 30km	66243	188538	2.85E-01	3.19E+00	1.33E-01	3.44E-02	4.30E-04	1.69E-03	7.04E-05	1.82E-05
≤ 50km	149733	438990	6.04E-01	6.91E+00	2.82E-01	7.33E-02	4.04E-04	1.57E-03	6.41E-05	1.67E-05
≤ 70km	256281	878432	1.01E+00	1.27E+01	5.13E-01	1.34E-01	3.93E-04	1.44E-03	5.84E-05	1.53E-05

465

Coll. means collapsed buildings; disp. means displaced residents.

Table 5. Ratio of losses during the Pollino sequence with respect to long term risk estimates (i.e., ratios of the cells in the columns coll., disp., injuries and fatalities of Table 3 divided by the corresponding values of Table 4).

01/01/2010	Distance	Coll.	Disp.	Injuries	Fatalities
	≤ 10km	0.76	0.82	0.73	0.73
	≤ 30km	0.82	0.86	0.78	0.78
	≤ 50km	0.86	0.89	0.81	0.82
	< 70km	0.90	0.92	0.85	0.85
25/10/2012	Distance	Coll.	Disp.	Injuries	Fatalities
	≤ 10km	3.26	2.95	3.53	3.50
	≤ 30km	2.16	2.02	2.12	2.11
	≤ 50km	1.77	1.69	1.69	1.69
	< 70km	1.54	1.46	1.42	1.41
26/10/2012	Distance	Coll.	Disp.	Injuries	Fatalities
	≤ 10km	49.99	42.56	55.59	54.79
	≤ 30km	26.16	22.54	26.14	25.89
	≤ 50km	17.67	15.60	17.14	16.99
	< 70km	12.68	10.90	11.39	11.25
21/07/2013	Distance	Coll.	Disp.	Injuries	Fatalities
	≤ 10km	1.54	1.50	1.59	1.59
	≤ 30km	1.29	1.27	1.26	1.26
	≤ 50km	1.20	1.19	1.15	1.16
	< 70km	1.16	1.14	1.09	1.09

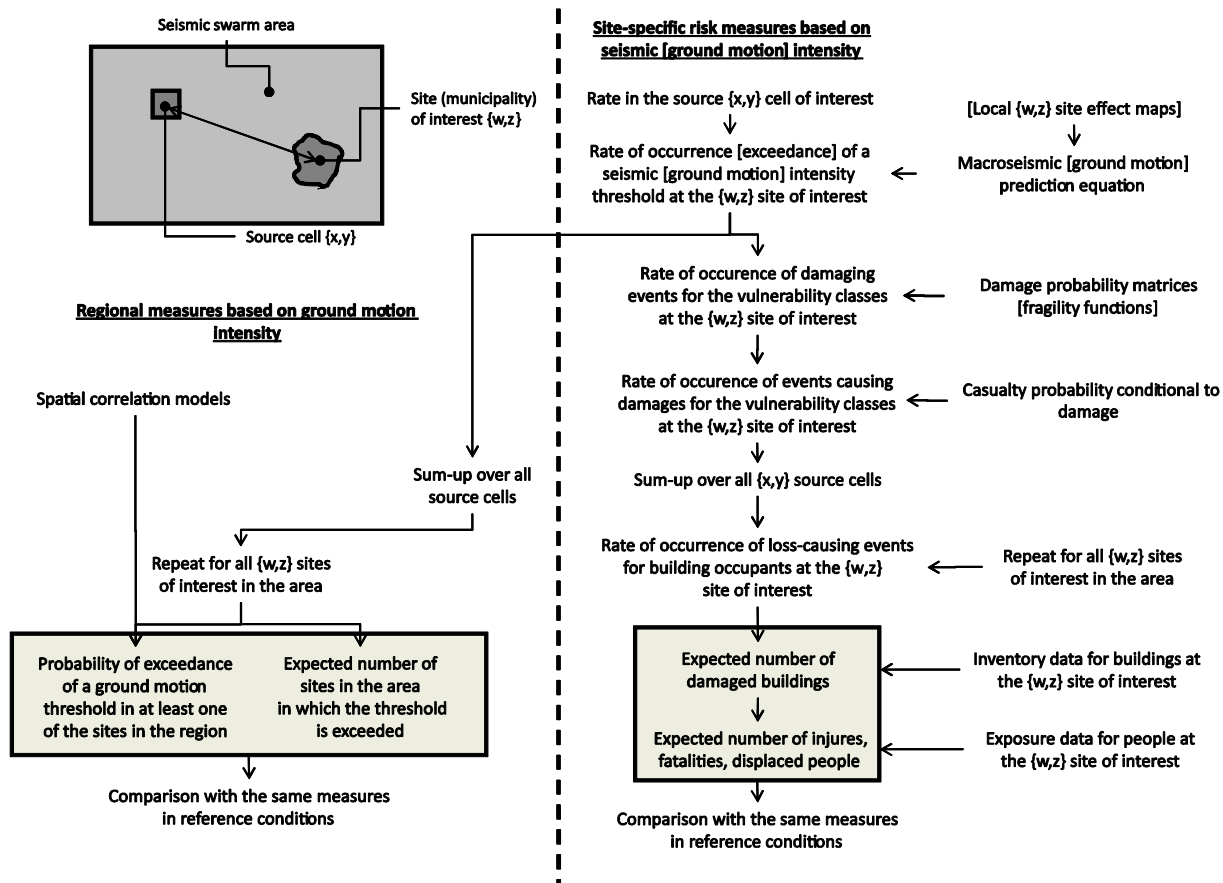


Figure 1. Sketch of the short-term risk assessment procedure.

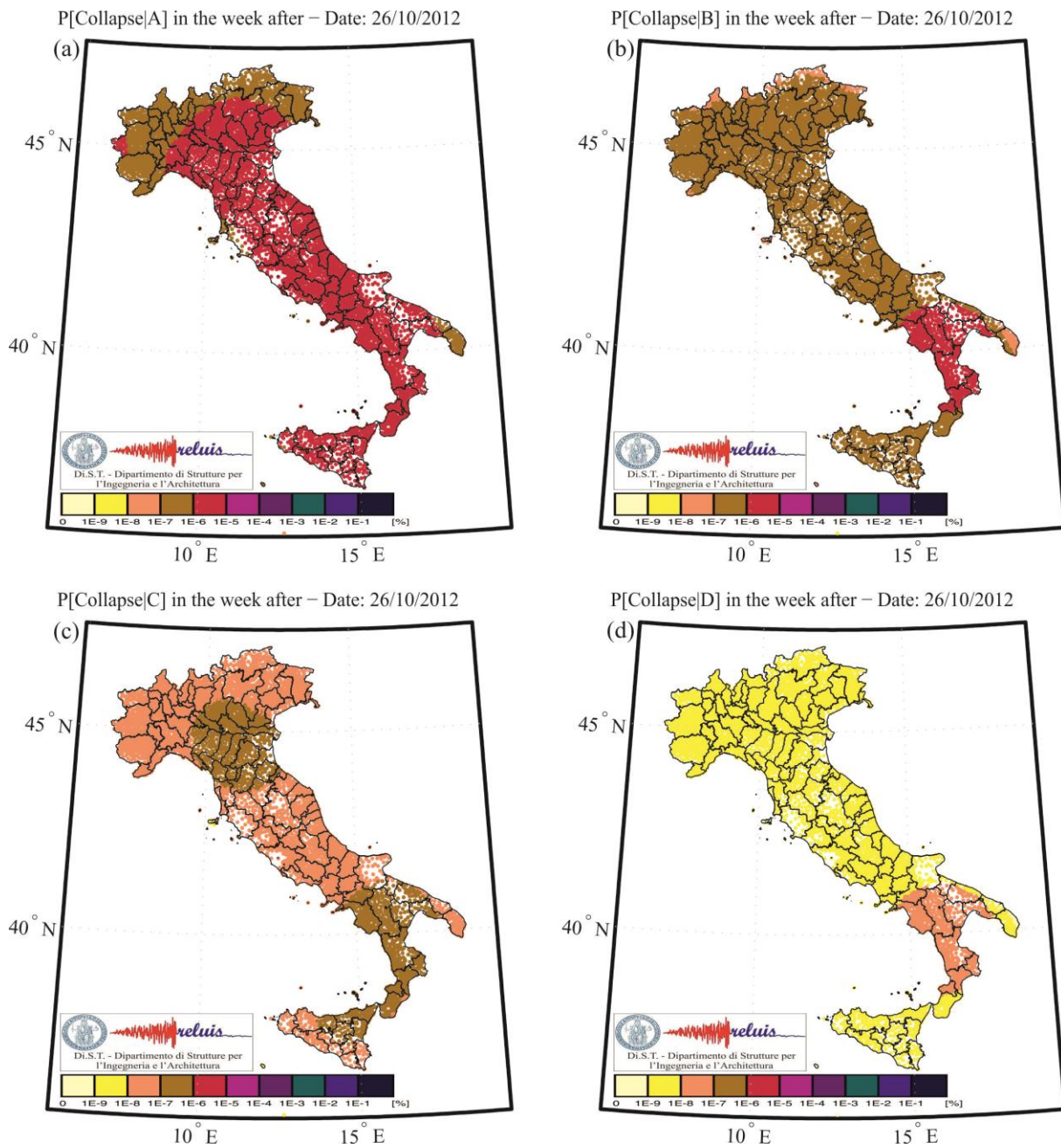


Figure 2. Weekly collapse probability per building vulnerability class after October 26th 2012.

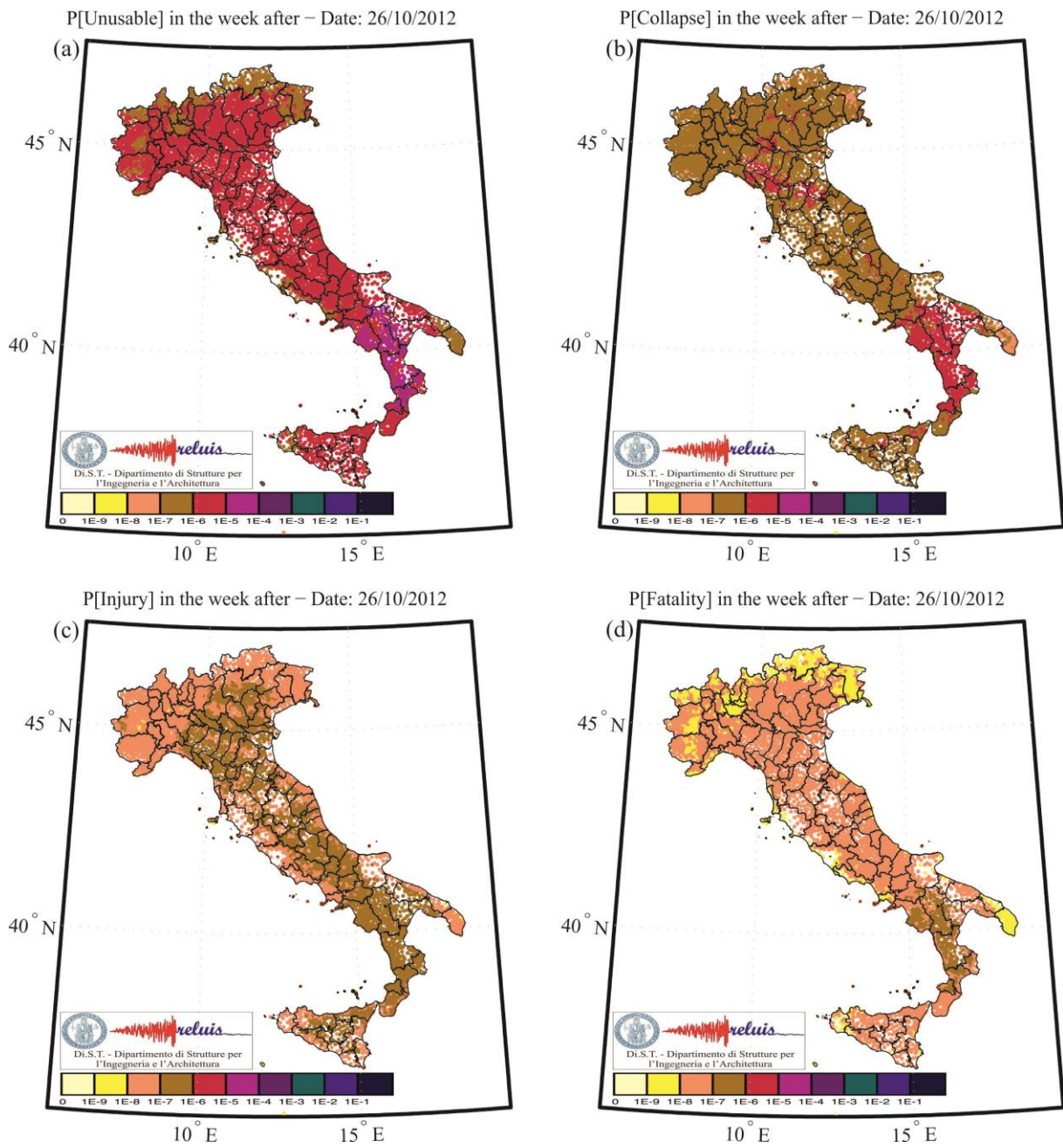


Figure 3. Weekly displaced, collapse, injury, and fatality probability after October 26th 2012.

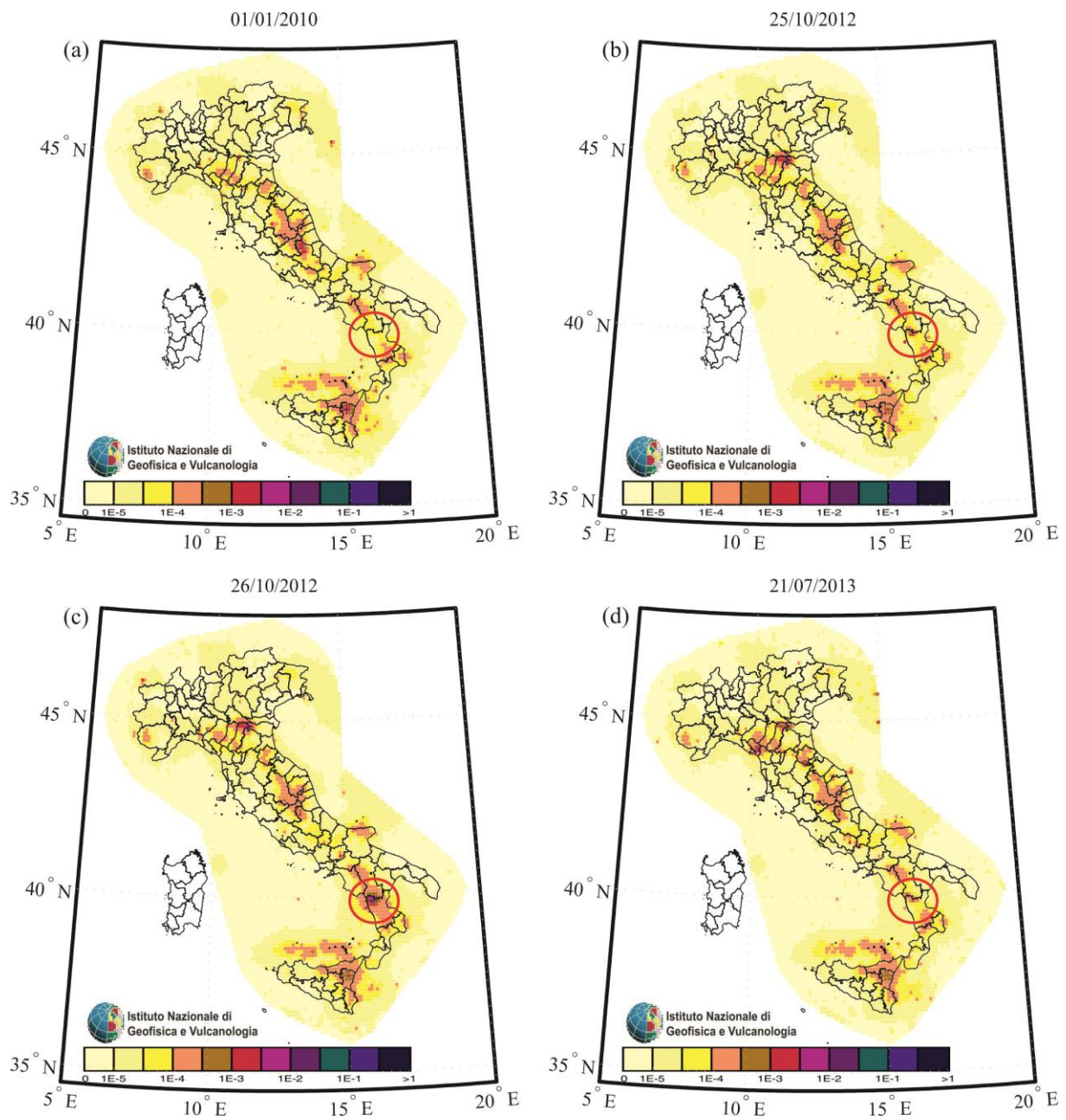


Figure 4. Seismic rates in terms of expected number of M4+ events per week estimated through OEF at the four considered instants of the Pollino (2012) sequence.

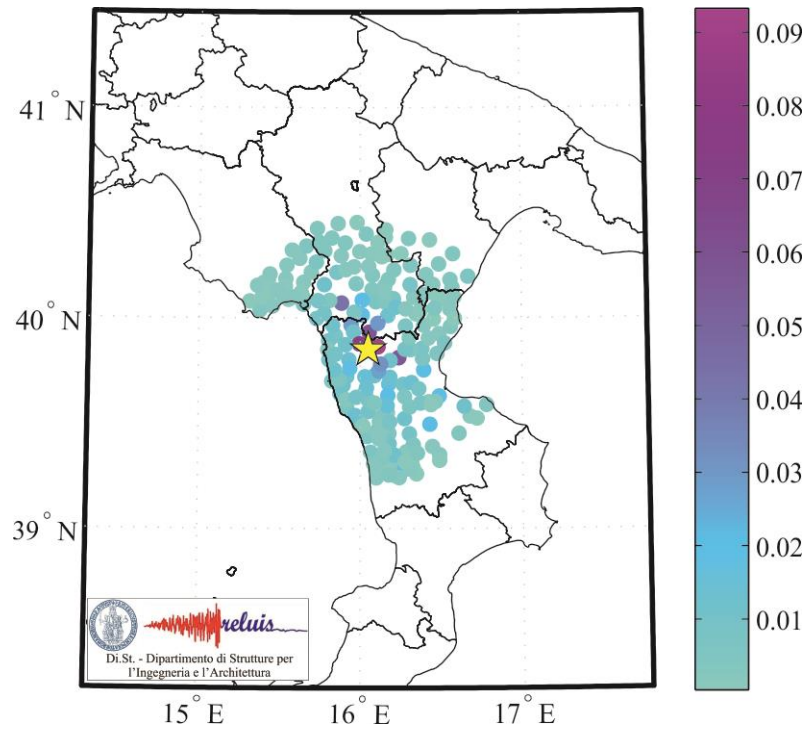


Figure 5. Considered municipalities within 70km (in radius) from the center of the Pollino sequence (star). The color of points is proportional to the expected number of fatalities, per municipality, in the week after 26/10/2012.

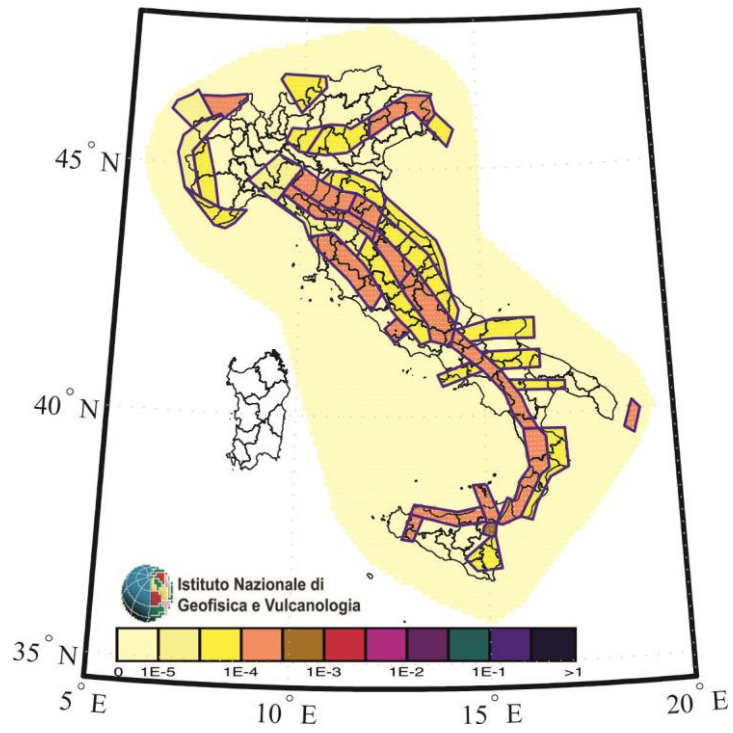


Figure 6. Weekly rates of M4+ events in one week adjusted from Barani et al. (2009) and seismic source model of Meletti et al. (2008).